coatings

MDPI

Article

Surface Characterization of Current Dental Ceramics Using Scanning Electron Microscopic and Atomic Force Microscopic Techniques

Katarzyna Kaczmarek [1,*], Bartlomiej Konieczny [2], Przemyslaw Siarkiewicz [3], Andrzej Leniart [1], Monika Lukomska-Szymanska [4], Slawomira Skrzypek [1] and Barbara Lapinska [4,*]

[1] Department of Inorganic and Analytical Chemistry, Faculty of Chemistry, University of Lodz, 12 Tamka St., 91-403 Lodz, Poland
[2] University Laboratory of Materials Research, Medical University of Lodz, 251 Pomorska St., 92-213 Lodz, Poland
[3] Institute of Polymer and Dye Technology, Lodz University of Technology, 12/16 Stefanowskiego St., 90-924 Lodz, Poland
[4] Department of General Dentistry, Medical University of Lodz, 251 Pomorska St., 92-213 Lodz, Poland
* Correspondence: katarzyna.kaczmarek@chemia.uni.lodz.pl (K.K.); barbara.lapinska@umed.lodz.pl (B.L.); Tel.: +48-42-635-57-83 (K.K.); +48-42-675-74-61 (B.L.)

Abstract: Dental ceramics is a highly esthetic material and its surface properties can impact its roughness, bonding properties, as well as strength and wear. The aim of the study is to analyze the surface characteristics by the determination of the roughness parameters of three dental ceramics used in computer-aided design/computer-aided manufacturing (CAD/CAM) technique: lithium disilicate (LS_2), zirconium oxide-reinforced lithium silicate (ZLS), and zirconium oxide (ZrO_2), prepared using two different processing techniques, polishing (self-glaze) and glazing with three different glazes. Both glass ceramics, pre-crystallized LS_2 and crystallized ZLS, were cut into disks, and the surface was ground and polished. Crystallization was performed for LS_2 samples, while ZrO_2 samples were fabricated using CAD/CAM and sintered. Then, the glaze was applied and the samples were reheated as per the manufacturer's instructions. The contact surface topographies of the tested ceramics were measured by atomic force microscopy (AFM) and the roughness parameters: average surface roughness (Ra), root-mean-square roughness (Rq), and surface area difference (SAD) were evaluated. Changes in the morphological characteristics of the tested ceramics were examined by scanning electron microscopy (SEM), and the surface chemical composition was determined by attenuated total reflection Fourier-transform infrared spectroscopy (FT—IR). In the spectroscopic analysis, a characteristic signal for ZrO_2 was obtained for ZLS samples. A significant decrease in surface roughness was observed after glazing in all tested ceramics ($p < 0.05$). The abstract should be an objective representation of the article and it must not contain results that are not presented and substantiated in the main text and should not exaggerate the main conclusions.

Keywords: dental ceramics; surface roughness; surface morphology; scanning electron microscopy; atomic force microscopy; attenuated total reflection Fourier-transform infrared spectroscopy; lithium disilicate; zirconium oxide-reinforced lithium silicate; zirconium oxide

Citation: Kaczmarek, K.; Konieczny, B.; Siarkiewicz, P.; Leniart, A.; Lukomska-Szymanska, M.; Skrzypek, S.; Lapinska, B. Surface Characterization of Current Dental Ceramics Using Scanning Electron Microscopic and Atomic Force Microscopic Techniques. *Coatings* **2022**, *12*, 1122. https://doi.org/10.3390/coatings12081122

Academic Editor: Devis Bellucci

Received: 4 July 2022
Accepted: 1 August 2022
Published: 5 August 2022

1. Introduction

For centuries, there has been a search for materials that would mimic and allow the permanent replacement of damaged dental hard tissues. The constantly rising patient demand for esthetic prosthetics has resulted in the development of dental prosthetics that do not have metal as a structural component for strengthening ceramics. The introduction of computer-aided design (CAD) and computer-aided manufacturing (CAM) of prosthetic restoration technology at the end of the 20th century, as well as high-strength materials

such as zirconium dioxide or lithium disilicate (LS_2), has enabled to expand the clinical applications of all-ceramic restorations [1]. Dental ceramics may differ in their chemical composition, structure, and method of preparation, and thus mechanical, optical, and esthetic properties [2–4]. In addition to their high strength, other desirable characteristics of ceramics have contributed to their wide clinical applications in dentistry. These characteristics include their stiffness, hardness, low thermal conductivity, and high fracture resistance in the oral cavity [5,6].

LS_2 glass ceramics are one of the highly esthetic ceramic dental materials. They are available in different forms, such as pre-crystallized blocks (blue blocks) [7].

After being subjected to crystallization, the milled prosthetic restoration undergoes a color change from bluish-gray to the natural shade of the tooth, acquiring appropriate optical properties similar to those of the natural tooth with an increase in mechanical strength from 130–150 MPa to 360 MPa. This material can be used in the fabrication of veneers, inlays, onlays, partial crowns, anterior and posterior crowns, three-unit bridges, and single restorations for implants [8].

Another type of esthetic glass ceramic material is zirconia-reinforced lithium silicate (ZLS) [9]. Its microstructure consists of a homogeneous glassy matrix with a crystalline component made of lithium metasilicate and lithium orthophosphate grains, together with tetragonal zirconia fillers added for increasing the strength. The crystallization of this ceramic material leads to the generation of LS_2. Due to the presence of a large proportion of glass, this ceramic material exhibits high translucency, opalescence, and fluorescence. ZLS is available in a pre-crystallized or crystallized form. This ceramic can be used in the fabrication of veneers, inlays, onlays, partial crowns, and anterior and posterior crowns [9].

Zirconium oxide (ZrO_2) is a ceramic material with the highest flexural strength (840–1200 MPa) [10,11]. Due to this property, ZrO_2 is suitable for fabricating not only single crowns or bridges, but also full-arch prosthetic restorations. The growing interest in ZrO_2 as a dental prosthetic material is also due to its high biocompatibility, which has been proven in both in vitro and in vivo tests [3,12]. Furthermore, zirconium accumulates a lesser number of bacteria than titanium alloys and a similar amount of tartar as the natural tooth [3,4,11,13–15].

After crystallization, the milled prosthetic restorations are polished or glazed. Glazing is the final step in restoration preparation and involves the application of another coating as an outer protective layer. Glazes are mainly thermally compatible, low-fusion aluminum silicate glasses that are rich in alkalis. Glazing results in a smooth and nonabsorbent surface, which is resistant to most chemical factors, such as acids and bases. It also prevents the wear of the material, while increasing the strength of restorations, protecting them against corrosion, and hindering the adhesion of other materials. After glazing, the restorations appear shiny and esthetic. The finished restorations are cemented in the patient's mouth using adhesive cement [16–19].

The surface characteristics of restorations influence their mechanical and chemical properties. Of these, surface roughness largely determines the quality of restorations [20]. Various dental instruments and finishing techniques (e.g., polishing and glazing) allow achieving a smooth surface to maximize the flexural strength of the restoration, minimize the risk of chipping or fracture, and reduce the abrasive wear of opposing teeth and restorations. Furthermore, these techniques maximize the biocompatibility of restorations by limiting the adherence of bacteria to their surface. Appropriate surface roughness should be maintained to allow a dental implant to quickly fuse with the jaw [21–23]. Finishing and polishing procedures also enhance the esthetics of milled CAD/CAM restorations, resulting in a glossy surface with similar reflection and refraction characteristics as those of natural teeth [24–29]. Therefore, it is essential to evaluate the microstructure and surface topography of dental ceramic materials. Unfortunately, the available literature has limited data on the abovementioned dental materials. This study collected the information on the topography of dental ceramic surface, complementing these deficiencies in the literature. These studies are potentially widely used in the work of dental practitioners, dental

technicians, and manufacturers of dental materials. The surface roughness is an important parameter characterizing the surface, closely related to the strength of adhesion between the various layers of ceramics, or between ceramics and tooth structures, as well as play a role in bacterial adhesion. Modifying the surface topography and its features allows for obtaining long-lasting, clinically sound ceramic restoration [20,30–33].

This study aims to analyze the surface characteristics of three CAD/CAM dental ceramic materials: LS_2, ZLS, and ZrO_2 ceramics. The materials' surfaces were prepared using two different processing techniques: polishing (self-glaze) and glazing. Atomic force microscopy (AFM) and scanning electron microscopy (SEM) were carried out to evaluate the surface topography of the studied materials, while their surface chemical composition was determined by attenuated total reflection (ATR) Fourier-transform infrared spectroscopy (FT—IR). It was hypothesized that differences in the surface topography among tested raw ceramic materials can be observed as well as among the materials' surfaces prepared using different finishing methods. Glazing causes a significant smoothing of the surface, which is manifested by a decrease in the value of the roughness parameters.

2. Materials and Methods

The study evaluated three types of dental ceramic materials (LS_2, ZLS, and ZrO_2 ceramics) and three glazes. Detailed information on the commercial ceramics used in the study is presented in Table 1.

Table 1. The materials used in the presented studies.

Product Name	Acronym Used in Paper	Type of Material	Translucency	Color/ Shade	Manufacturer	LOT Number
IPS e. max® CAD	LS_2	lithium disilicate glass ceramic	HT	A20/B40	Ivoclar Vivadent, Schaan, Liechtenstein	X36997
Celtra® Duo	ZLS	zirconia-reinforced lithium silicate	HT	A2/C14	DeguDent GmbH, Hanau-Wolfgang, Germany	16005937
ZIRCONIA	ZrO_2	zirconium oxide	HT	White	Bloomden Bioceramics Co., Ltd., Hunan, China	BL180712001
Celtra®Ceram	CC	leucite-reinforced feldspathic ceramic	-	-	DeguDent GmbH, Hanau-Wolfgang, Germany	18004711
IPS e.max® Ceram	IC	fluorapatite veneering ceramic	-	-	Ivoclar Vivadent, Schaan, Liechtenstein	Z00MCX
IPS Ivocolor® Glaze Paste	IIG	alkali aluminosilicate glass	-	-	Ivoclar Vivadent, Schaan, Liechtenstein	Y10534

LS_2 and ZLS ceramic blocks were cut using an SYJ-200 automatic precision cutting machine (Shenyang Kejing Automation Equipment Co., Ltd., Shenyang, China), equipped with a diamond wheel with cutting speed 1 mm/min, into 5 mm thick slices, obtaining 20 samples of each ceramics. All samples were subsequently polished with 500, 800, and 1500 grit silicon carbide (SiC) water-based paper. After polishing, the samples were cleaned with distilled water in an ultrasonic bath (Intersonic S.C., Olsztyn, Poland) for 10 min and dried for 24 h at room temperature. For LS_2 ceramic samples, crystallization was carried out as per the manufacturer's instructions.

The samples of ZrO_2 ceramics were processed using the CAD/CAM method, with the Amann Girrbach system consisting of Ceramill Motion 4 axis milling machine (Amann Girrbach, Koblach, Austria) and Fusion 360 software (Autodesk Inc., 2.0.9719, San Rafael, CA, USA). After milling and annealing, the 20 samples were designed in the shape of a cylinder with a diameter of 2 cm. Heating was carried out in an oven (Ceramill Therm 3, Amann Girrbach, Koblach, Austria) for 10 h at a temperature of 1450 °C (8 °C/h, the final temperature was maintained for 2 h and then the samples were automatically cooled to about 200 °C).

Thus, the prepared samples of each tested ceramics were randomly divided into four study groups (n = 5). Group 1 included samples without additional glazing, while in groups 2 to 4, the contact surface of ceramic samples was covered with a thin layer of

glaze (CC, IC, or IIC), heated in the oven (AG Programat P3000, Ivoclar Vivadent, Schaan, Liechtenstein) for 3 h at 800 °C, and then cooled to room temperature.

2.1. Measurement of Surface Roughness

Surface roughness was measured with an atomic force microscope (AFM; Dimension Icon, Bruker, Santa Barbara, CA, USA) controlled by NanoScope 9.0 software (Bruker, Santa Barbara, CA, USA) and expressed as parameters Rq (the root-mean-square average of height deviations taken from the mean image data plane), Ra (the arithmetic average of absolute values of surface height deviations measured from the mean plane), and SAD (surface area difference referred to the difference between the three-dimensional (3D) surface area of an analyzed region and its two-dimensional (2D) footprint area). Scanning was carried out in tapping mode using a TESPA silicon probe (NanoWorld, Neuchâtel, Switzerland), which consisted of a rectangular cantilever with a nominal spring constant of 42 N/m and a nominal resonance frequency of 320 kHz, and a pyramidal tip with a nominal radius of 7 nm. The surface parameters measured based on the AFM measurements were analyzed using NanoScope Analysis 1.5 software (Bruker, Santa Barbara, CA, USA). For each sample, surface roughness was measured at three different points. For each area, scans with a size of 20 μm × 20 μm and 1 μm × 1 μm were made, and for each size, a downward and upward scan were also made. Prior to the AFM measurement, the samples were purged in an argon stream.

2.2. Scanning Electron Microscopy (SEM) Observation

A scanning electron microscope (Phenom G2 Pure, FEI Company, The Netherlands) was used to observe the surface of tested ceramics before (polished/milled) and after glazing. During analysis, the ceramics were fixed on an SEM pin stub using copper tape. SEM images were acquired at a magnification of 250×, using a high-sensitivity backscattered electron detector operating at an accelerating voltage of 5 kV.

2.3. Fourier-Transform Infrared Spectroscopy with Attenuated Total Reflectance Sensor (FT—IR-ATR) Measurements

FT—IR studies were carried out to analyze the glazed coating and identify the particles included in the ceramics. The ATR FT—IR measurements were obtained using a Nicolet 6700 spectrometer (Thermo Fisher Scientific, Waltham, MA, USA) in the range of 400–4000 cm^{-1}. Samples were measured directly, and an average of 16 scans was obtained. All samples were examined in three different regions to ascertain the correctness of the obtained data.

2.4. Statistical Analysis

Statistical analyses were performed using Microsoft Excel 2020 and PQStat v 1.6.8.384 (PQStat Software, Poznan, Poland). Because the distribution of data was not normal (Kolmogorov–Smirnov test) and variances among specimens were unequal (Levene's test), nonparametric methods were used [34]. Data were expressed as medians with interquartile ranges. To determine whether the tested ceramics differed in their surface roughness, a Wilcoxon signed-rank test was run for each paired group (i.e., same base, different glaze type). Furthermore, to find whether the results were material-dependent, a Kruskal–Wallis test was performed. A Steel–Dwass post hoc test was used to detect the differences between the groups [28]. A simple regression analysis was carried out to determine the association between surface roughness and the type of tested ceramics. For each of the tests, the confidence level was assumed at $\alpha < 0.05$. The results were coded based on the requirements of the method.

3. Results

Figure 1 presents some 2D AFM images obtained for 20 μm × 20 μm area of the tested ceramic surfaces before and after glazing. The surface of ceramic samples showed mod-

erate irregularity with numerous peaks and valleys, while glazed samples had relatively smooth surfaces with glaze crystallites visible in some places. The AFM images obtained for 20 µm × 20 µm areas were presented as to enable further comparison and correlation with the SEM images. The surface roughness parameters (Rq, Ra, and SAD) of the tested samples are shown in Table 2. In order to characterize the surface of tested samples and average the results, measurements were made at several points on their surface for 1 µm × 1 µm and 20 µm × 20 µm areas. The measured parameters were expressed as medians with interquartile ranges. It can be deduced from the table that the values of roughness parameters differed significantly depending on the type of samples. In the case of raw samples, the lowest Rq values (for 20 µm × 20 µm area) were obtained for LS_2 (83.7 [76.4–189.8] nm), while the highest for ZLS (268.5 [244.8–316.0] nm). The Wilcoxon signed-rank test revealed a significant difference in surface roughness (Rq, Ra, and SAD) between the tested materials ($p < 0.05$).

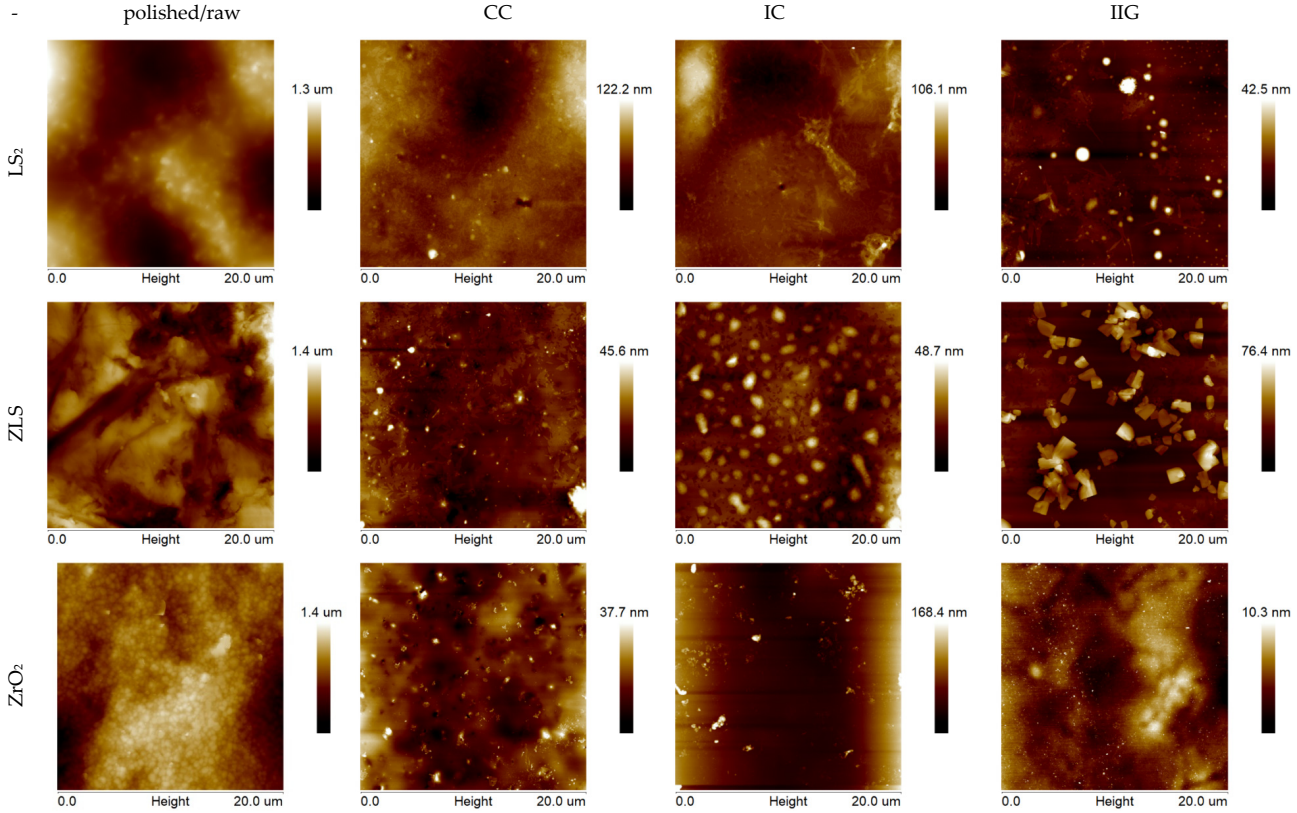

Figure 1. AFM 2D images (area 20 µm × 20 µm) of the tested ceramic surfaces before and after glazing.

Table 2. The surface roughness of the tested ceramics.

Samples	Rq [nm]		Ra [nm]		SAD [%]	
	Area 20 µm × 20 µm	Area 1 µm × 1 µm	Area 20 µm × 20 µm	Area 1 µm × 1 µm	Area 20 µm × 20 µm	Area 1 µm × 1 µm
LS_2	83.0 [73.6–116.0]	7.0 [4.01–8.2]	64.0 [52.7–122.45]	5.6 [3.0–5.7]	0.62 [0.23–1.09]	1.46 [1.42–1.48]
LS_2-CC	10.2 [7.4–17.6]	1.3 [1.1–1.9]	6.6 [5.0–11.4]	0.9 [0.9–1.3]	0.14 [0.12–0.21]	0.93 [0.69–1.11]
LS_2-IC	9.0 [6.7–11.2]	1.8 [0.8–2.2]	6.6 [4.5–7.8]	0.9 [0.5–1.6]	0.12 [0.09–0.16]	0.65 [0.55–1.07]
LS_2-IIG	7.8 [7.3–8.4]	1.3 [0.9–3.0]	4.8 [4.1–5.3]	1.0 [0.5–2.0]	0.11 [0.08–10]	0.58 [0.31–8.43]
ZLS	268.5 [244.8–316.0]	16.1 [13.1–28.5]	213.5 [177.8–250.3]	12.2 [10.3–20.9]	11.20 [10.78–15.33]	11.70 [4.09–12.33]
ZLS-CC	8.9 [7.2–12.7]	1.7 [0.9–3.1]	5.8 [4.6–7.6]	1.1 [0.6–2.5]	0.15 [0.09–0.25]	0.66 [0.45–1.61]
ZLS-IC	15.6 [13.0–44.8]	2.4 [1.5–3.8]	10.1 [8.0–18.8]	1.4 [1.0–2.8]	0.26 [0.12–0.54]	0.80 [0.54–1.16]
ZLS-IIG	14.8 [11.3–22.5]	1.0 [0.4–3.5]	9.1 [8.1–13.9]	0.8 [0.2–2.6]	0.30 [0.28–0.54]	0.39 [0.34–1.34]
ZrO_2	154.5 [103.0–270.0]	26.4 [22.9–30.0]	119.3 [76.7–219.0]	20.6 [18.6–23.9]	7.87 [7.85–10.03]	8.06 [7.87–8.43]
ZrO_2-CC	12.1 [10.0–17.0]	1.8 [1.1–3.8]	9.6 [6.6–10.3]	1.2 [0.7–2.4]	0.25 [0.11–0.38]	1.36 [0.57–1.57]
ZrO_2-IC	29.1 [20.1–33.2]	1.0 [0.6–1.6]	12.7 [10.8–14.4]	0.6 [0.4–0.9]	0.69 [0.32–0.78]	0.72 [0.38–1.36]
ZrO_2-IIG	1.9 [1.6–4.5]	0.4 [0.3–1.0]	1.3 [1.2–3.4]	0.3 [0.2–0.5]	0.03 [0.01–0.05]	0.39 [0.26–0.82]

Rq = root-mean-square average roughness; Ra = average roughness; SAD = surface area difference.

Box plots were presented for a more complete illustration of the changes observed in the values of roughness parameters both within and between the groups of the tested samples (Figures 2–4).

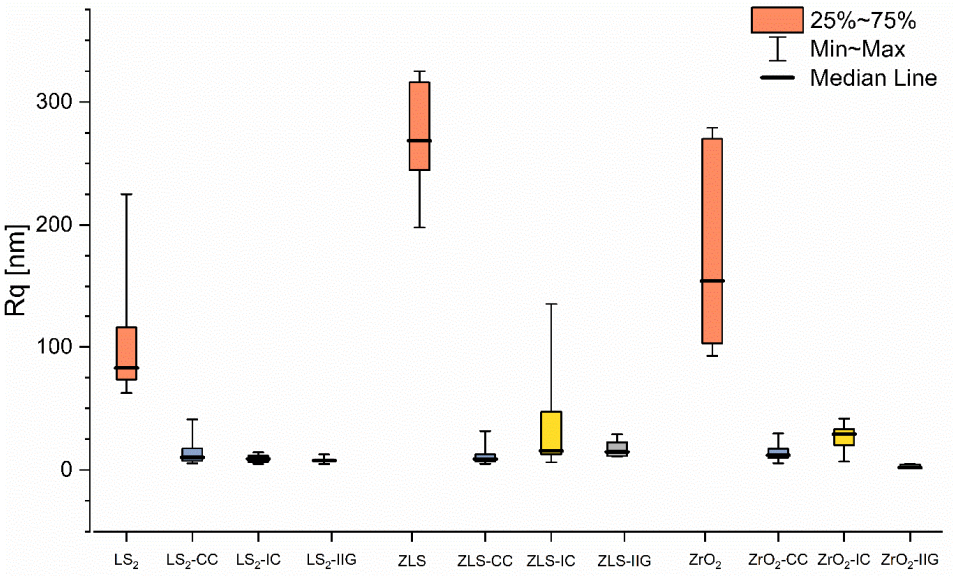

Figure 2. The root-mean-square average roughness (Rq) data for 20 μm × 20 μm area of the tested ceramic surfaces before and after glazing.

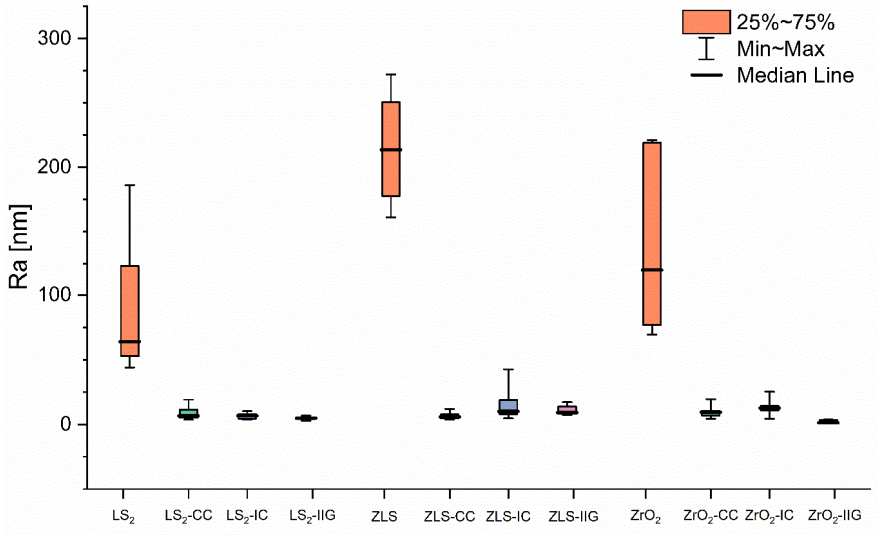

Figure 3. The average roughness (Ra) data for 20 μm × 20 μm area of the tested ceramic surfaces before and after glazing.

The interquartile range represented the region between the 25th (25%, lower quartile) and 75th percentile (75%, upper quartile). MIN denoted the lowest value in the dataset, while MAX denoted the highest value.

The SEM images obtained before and after glazing of the surface of each ceramic material are shown in Figure 5. The images acquired at a magnification of 250× showed that the glazed ceramic specimens were smoother, more uniform, and free of larger particles, compared to the raw specimen. The SEM analysis confirmed the results obtained from the AFM analysis.

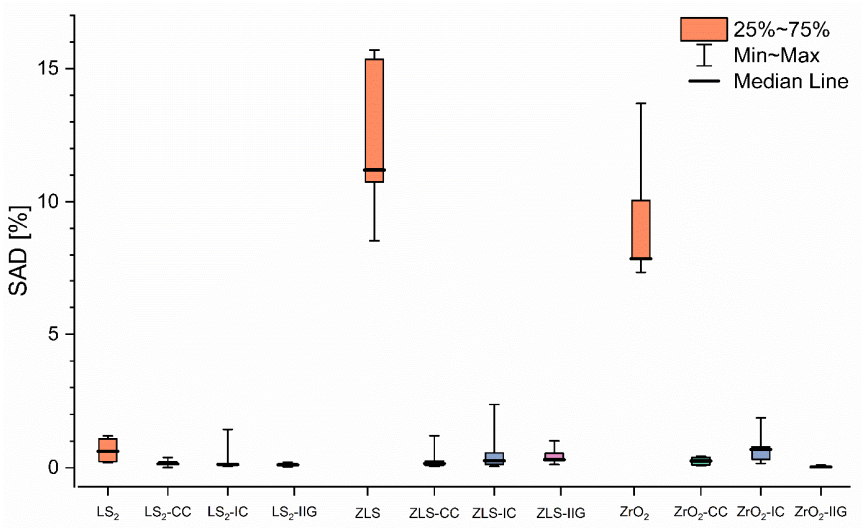

Figure 4. The surface area difference (SAD) data for 20 μm × 20 μm area of the tested ceramic surfaces before and after glazing.

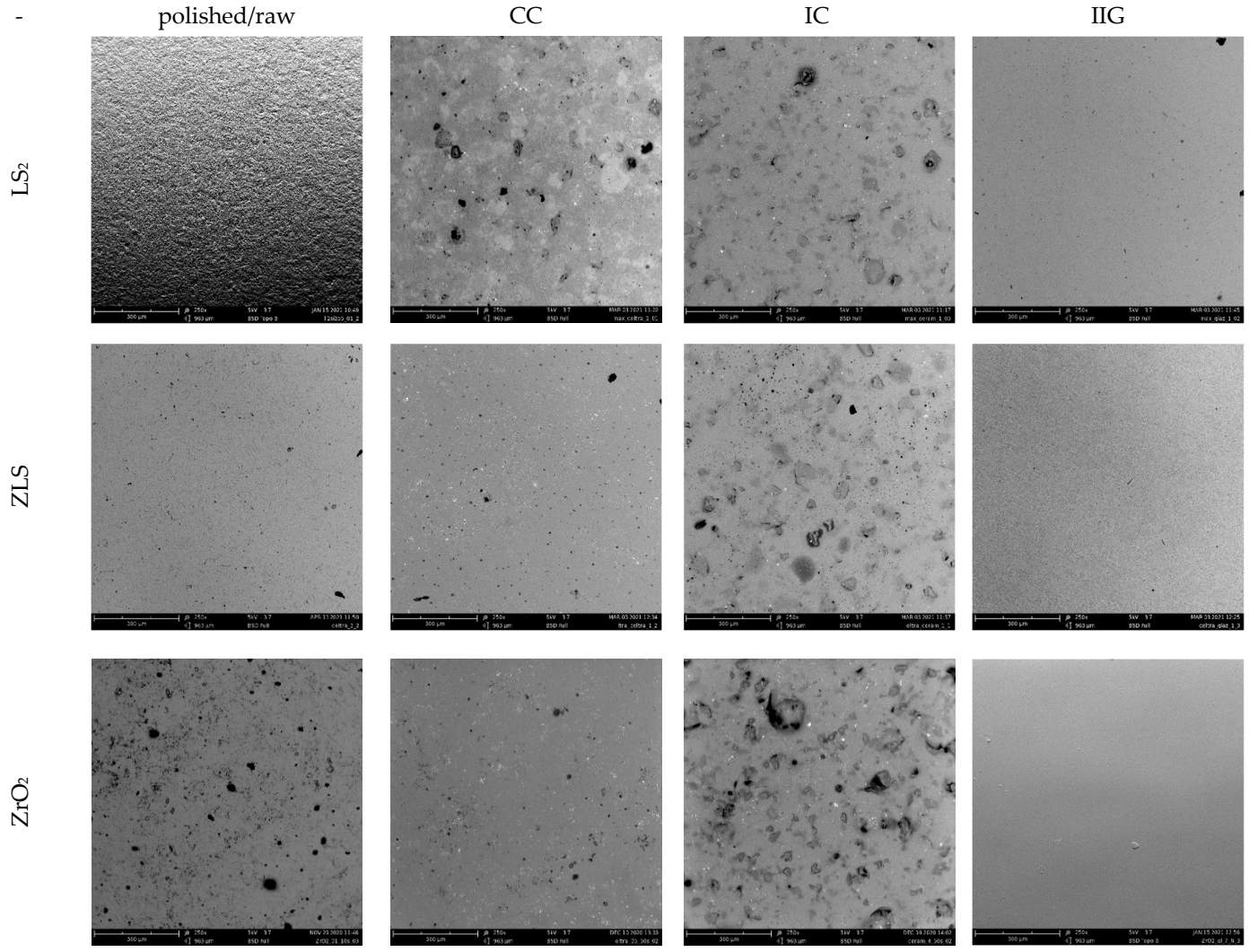

Figure 5. SEM images (magnification 250×) of the tested ceramic surfaces after polishing (raw) and after glazing with CC, IC, and IIG glazes.

When samples were studied by FT—IR, the characteristic signal of ZrO_2 (608 cm^{-1}) was noticed for ZrO_2 and ZLS samples (Figure 6). On the other hand, this band was not seen for LS_2 samples, which did not have ZrO_2 in their composition.

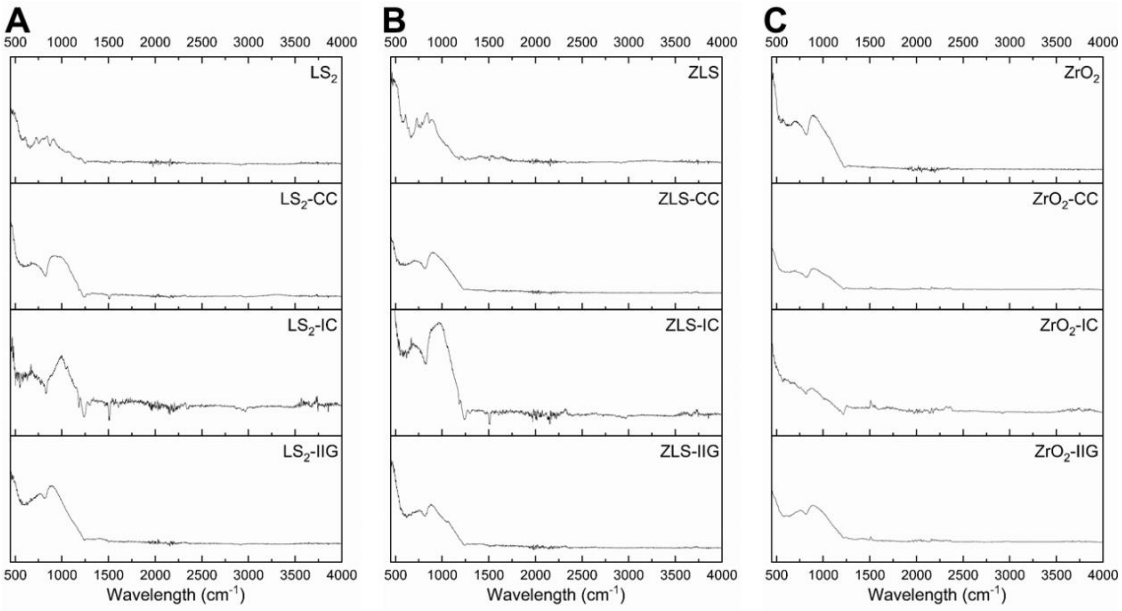

Figure 6. FT—IR spectra of the tested ceramics: (**A**) LS_2 ceramics; (**B**) ZLS ceramics; (**C**) ZrO_2 ceramics; before and after glazing with CC, IC, and IIG glazes.

4. Discussion

AFM is one of the best techniques used to evaluate the surface topography/morphology of dental materials [35,36]. In this study, based on the obtained AFM topographic images, the roughness parameters of the tested dental ceramics were determined for two different scan sizes. Surface roughness is an important factor of all dental materials, including glass ceramics [20,37,38]. It affects the final visual effect of restorations as well as bacterial adhesion. For bonding to hard dental tissues, ceramic restoration with high roughness on the inner surface is preferred, since it contributes to the improved durability of the bond [35,39]. On the contrary, the outer surface of dental ceramic restoration is required to be as smooth as possible to prevent or reduce plaque accumulation, bacterial adhesion, gingival irritation, or secondary caries [40,41].

The cited literature presents different values of dental ceramic surface roughness parameters, which is mainly due to the use of different polishing procedures and final polishing materials. The value of Ra determined for lithium silicate-based glass ceramics for an area of 50 μm × 50 μm after sandblasting ranged from 227 to 867.8 nm [8]. However, when a liquid emulsion with a grain size of 6 and 0.04 μm was used for the fine polishing of the surface [35], the values of the roughness parameters were quite low. On the other hand, when a 600 SiC sandpaper was used, the values of the parameters obtained were higher [16].

In the present study, glazing significantly smoothed the surface of the tested materials. The lowest values of all tested roughness parameters (Rq, Ra, and SAD) were obtained for ZrO_2-IIG (Ra = 1.3 nm [1.2–3.4] for 20 μm × 20 μm area), whereas the highest values of these roughness parameters were obtained for ZrO_2-IC (Ra = 12.7 nm [10.8–14.4] for 20 μm × 20 μm area). All roughness parameters were smaller for the 1 μm × 1 μm scanning areas. The decrease in the values of roughness parameters with the size of the scanning area is typical for the AFM measurements [42]. The present study used AFM scans of 20 μm × 20 μm and 1 μm × 1 μm area. There is no established protocol in the literature concerning the scan size of dental materials: it varies between 10 μm × 10 μm [43],

20 µm × 20 µm [44–46], and 50 µm × 50 µm [8,35]. However, the roughness is scale-dependent and increases when a larger area is studied.

For glazed ceramic materials used in the study, the roughness parameters were lower in comparison to the ones of polished samples. However, the literature presents with contrasting findings. For LS_2 ceramics, based on AFM measurements, Pantic et al. [35] determined Ra and Rq values of 2.5 and 2.5 nm (for polished samples) and 17.2 and 21.8 nm (for glazed samples), respectively, for an area of 50 µm × 50 µm. For ZLS and LS_2 ceramics, the value of Ra ranged from 35.73 to 55.74 nm after polishing and from 71.67 to 85.91 nm after glazing, for an area of 60 µm × 60 µm [16]. Due to the fact that AFM measurements are of small scale (local measurements), they are characteristic of a given measurement area. Therefore, the data obtained from AFM provide information about the properties of the sample only for a given location. Thus, the obtained topographic results have a large dispersion, as evidenced by large differences in values between the lower and upper quartile (Figures 2–4).

Contradictory results were also presented by Dal Piva et al. [47], who reported that, regardless of ceramic material (ZrO_2 or ZLS), glazed surfaces were rougher than the polished ones. Moreover, they observed that ZLS ceramics, glazed or polished, had a more homogenous surface than ZrO_2 ceramics. However, in this case, such contrasting outcomes could result from the different glaze application technique used in the studies as well as surface roughness measurement methods [44].

The analysis of the influence of the substrate on the glazing effect indicated a decrease in the values of roughness parameters in the case of ZLS-CC, LS_2-IC, and ZrO_2-IIG samples. When comparing the results obtained for one base ceramics after the application of IIG glaze, the smoothest surfaces were observed for both LS_2 and ZrO_2 ceramics. A similar dependence was noticed for ZLS when the CC glaze was applied.

This study showed that glazing applied as a finishing treatment smoothened the surface by filling various types of unevenness and pores on it, as can be seen in the AFM images (Figure 1). From an esthetic point of view, glazing is recommended to obtain glossy all-ceramic restorations [26–28,35,48]. Another important aspect of finishing the outer surface of ceramic restoration is to limit bacterial adhesion and plaque accumulation by modelling the topography and hydrophobicity of the surface [38]. It was noted that dental ceramic finishing procedures (polishing and/or glazing) may result in surface free energy (SFE) changes [49]. Oral microbiota preferentially adheres to high SFE substrates (hydrophilic ones), therefore keeping ceramic SFE low would attract fewer bacteria. Yet, the hydrophobic surface of ceramic materials, although antibacterial, can have increased roughness [47]. This issue needs further investigation, as it was reported that polished LS_2 with higher SFE presented with similar volume of bacteria adhesion as hydrophobic ZrO_2 (with lower SFE) [50], suggesting that oral fluids may change SFE of some substrates [40]. As can be seen in Figures 2–4, comparatively shorter box plots were obtained for glazed samples, which proved that their surface topography was more homogeneous. This was confirmed by both AFM and SEM images. The SEM images produces no quantitative information in the Z direction, whereas AFM besides the nanometer resolution in the plane (x, y), provides additional information along the vertical axis (Z) [51].

The FT-IR analysis of studied dental ceramics showed a characteristic signal of ZrO_2 for both ZrO_2 and ZLS samples. Furthermore, in the literature, this signal has been described as characteristic of ZrO_2 nanoparticles [52]. In our opinion, FT-IR can be used as a tool in advanced studies of dental materials [36].

There are some limitations to the presented methodology, strictly resulting from the applied research methods, i.e., AFM, SEM, or FT-IR. The main limitation of this methodology is the shape and size of the sample. The size of the sample is to resemble the dimensions of the tooth. Too large sample could not fit into the measuring chamber, too small a sample due to further testing could be difficult to attach to a rack. Real non-conductive samples, i.e., ceramics, have some limitations in obtaining SEM images at high magnifications.

The AFM seems to be very useful for the studies of biomaterials, as it has some important advantages, such as minimal sample preparation, high resolution, and visualization of a three-dimensional image of the surface [36,53]. Further studies should focus on the implementation of AFM technique in investigating surface roughness of dental restorative materials (e.g., resin composites and dental ceramics) under the challenging conditions of oral cavity and after the application of dentifrices or bleaching agents [54–56].

To sum up, it can be concluded that glazing reduced the roughness coefficients, thus significantly smoothened the surface of the tested materials. This is a desired effect for the outer surface of dental restorations made of, e.g., ceramics, for both, esthetic and hygienic reasons.

5. Conclusions

This study analyzed the surface roughness of dental ceramic materials by applying SEM and AFM techniques. In addition, qualitative analyses of the ceramic surfaces were performed using FT-IR. Several studies have emphasized the importance of using more than one method for the evaluation of surface characteristics, i.e., SEM, AFM, and FT-IR, for the qualitative analyses of the ceramic surfaces, and applying AFM the quantitative analyses. The Rq, Ra, and SAD parameters are frequently chosen for the quantitative description of surface roughness. The determined values of Rq, Ra, and SAD showed a significant decrease in the surface roughness of all tested ceramics after glazing. An association was observed between surface roughness and the type of ceramic material tested.

Author Contributions: Conceptualization, K.K., S.S. and M.L.-S.; methodology, M.L.-S.; software, A.L.; validation, A.L., B.L. and S.S.; formal analysis, K.K.; investigation, K.K., B.K. and P.S.; resources, B.L.; data curation, A.L.; writing—original draft preparation, K.K.; writing—review and editing, B.L., S.S. and M.L.-S.; visualization, K.K. and A.L.; supervision, S.S.; project administration, S.S. and M.L.-S.; funding acquisition, M.L.-S. All authors have read and agreed to the published version of the manuscript.

Funding: This research was funded by the National Centre for Research and Development (Warsaw, Poland) within the grant InterChemMed (WND-POWR.03.02.00-00-I029/16-01).

Institutional Review Board Statement: Not applicable.

Informed Consent Statement: Not applicable.

Data Availability Statement: Data sharing is not applicable to this article.

Conflicts of Interest: All authors declare no conflict of interest in this paper.

References

1. Denry, I.; Kelly, J.R. Emerging Ceramic-based Materials for Dentistry. *J. Dent. Res.* **2014**, *93*, 1235–1242. [CrossRef] [PubMed]
2. Denry, I.; Holloway, J. Ceramics for dental applications: A review. *Materials* **2010**, *3*, 351–368. [CrossRef]
3. Daou, E.E.; Al-Gotmeh, M. The Zirconia Restoration Properties: A Versatile Restorative Material. *Dentistry* **2014**, *4*, 1000219. [CrossRef]
4. Warreth, A.; Elkareimi, Y. All-ceramic restorations: A review of the literature. *Saudi Dent. J.* **2020**, *32*, 365–372. [CrossRef]
5. Mörmann, W. The evolution of the CEREC system. *J. Am. Dent. Assoc.* **2006**, *137*, 7S–13S. [CrossRef]
6. Sumi, T.; Braian, M.; Shimada, A.; Shibata, N.; Takeshita, K.; Vandeweghe, S.; Coelho, P.G.; Wennerberg, A.; Jimbo, R. Characteristics of implant-CAD/CAM abutment connections of two different internal connection systems. *J. Oral Rehabil.* **2012**, *39*, 391–398. [CrossRef]
7. Azar, B.; Eckert, S.; Kunkela, J.; Ingr, T.; Mounajjed, R. The marginal fit of lithium disilicate crowns: Press vs. CAD/CAM. *Braz. Oral Res.* **2018**, *32*, 1–7. [CrossRef]
8. Bebsh, M.; Haimeur, A.; França, R. The Effect of Different Surface Treatments on the Micromorphology and the Roughness of Four Dental CAD/CAM Lithium Silicate-Based Glass-Ceramics. *Ceramics* **2021**, *4*, 34. [CrossRef]
9. Zarone, F.; Ruggiero, G.; Leone, R.; Breschi, L.; Leuci, S.; Sorrentino, R. Zirconia-reinforced lithium silicate (ZLS) mechanical and biological properties: A literature review. *J. Dent.* **2021**, *109*, 103661. [CrossRef]
10. Bączkowski, B.; Ziębowicz, A.; Ziębowicz, B.; Wojtyńska, E.; Mierzwińska-Nastalska, E. Assessment of the microhardness and roughness of zirconium oxide used in the production of individual ceramic implant abutments. *Protet. Stomatol.* **2020**, *70*, 33–42. [CrossRef]

11. Fu, L.; Engqvist, H.; Xia, W. Glass-ceramics in dentistry: A review. *Materials* **2020**, *13*, 1049. [CrossRef]
12. Baltatu, M.S.; Vizureanu, P.; Sandu, A.V.; Munteanu, C.; Istrate, B. Microstructural analysis and tribological behavior of Ti-based alloys with a ceramic layer using the thermal spray method. *Coatings* **2020**, *10*, 1216. [CrossRef]
13. Li, R.W.K.; Chow, T.W.; Matinlinna, J.P. Ceramic dental biomaterials and CAD/CAM technology: State of the art. *J. Prosthodont. Res.* **2014**, *58*, 208–216. [CrossRef] [PubMed]
14. Baltatu, M.S.; Vizureanu, P.; Sandu, A.V.; Florido-Suarez, N.; Saceleanu, M.V.; Mirza-Rosca, J.C. New titanium alloys, promising materials for medical devices. *Materials* **2021**, *14*, 5934. [CrossRef] [PubMed]
15. Focsaneanu, S.C.; Vizureanu, P.; Sandu, A.V.; Ciobanu, G.; Baltatu, S.M.; Vlad, D. Experimental study on the influence of zirconia surface preparation on deposition of hydroxyapatite. *Rev. Chim.* **2019**, *70*, 2273–2275. [CrossRef]
16. Shibasaki, P.; Cavalli, V.; Oliveira, M.; Barbosa, J.; Boriollo, M.; Martins, L. Influence Of Surface Treatment On The Physical Properties And Biofilm Formation Of Zirconia-Reinforced Lithium Silicate Ceramics: In Vitro Trial. *Int. J. Prosthodont.* **2021**. [CrossRef]
17. Özyılmaz, Ö.Y.; Özel, G.S.; Bevek, S.; Ahmet, O. Effects of Glazing Procedures on the Color Stability of Conventional and CAD/CAM Hybrid Ceramics: A Comparative Study. *Meandros Med. Dent. J.* **2019**, *20*, 209–219. [CrossRef]
18. Singh, R.G.; Li, K.C.; Lyons, K.M.; Waddell, J.N. Effect of Two Brands of Glaze Material on the Flexural Strength and Probability of Failure of High Translucent Monolithic Zirconia. *Materials* **2021**, *14*, 7022. [CrossRef] [PubMed]
19. Cattell, M.J.; Chadwick, T.C.; Knowles, J.C.; Clarke, R.L. The development and testing of glaze materials for application to the fit surface of dental ceramic restorations. *Dent. Mater.* **2009**, *25*, 431–441. [CrossRef]
20. Rashid, H. The effect of surface roughness on ceramics used in dentistry: A review of literature. *Eur. J. Dent.* **2014**, *8*, 571–579. [CrossRef]
21. Kowalski, J.; Lapinska, B.; Nissan, J.; Lukomska-Szymanska, M. Factors Influencing Marginal Bone Loss around Dental Implants: A Narrative Review. *Coatings* **2021**, *11*, 865. [CrossRef]
22. Lo Giudice, A.; Ronsivalle, V.; Grippaudo, C.; Lucchese, A.; Muraglie, S.; Lagravère, M.O.; Isola, G. One Step before 3D Printing—Evaluation of Imaging Software Accuracy for 3-Dimensional Analysis of the Mandible: A Comparative Study Using a Surface-to-Surface Matching Technique. *Materials* **2020**, *13*, 2798. [CrossRef] [PubMed]
23. Lo Giudice, A.; Leonardi, R.; Ronsivalle, V.; Allegrini, S.; Lagravère, M.; Marzo, G.; Isola, G. Evaluation of pulp cavity/chamber changes after tooth-borne and bone-borne rapid maxillary expansions: A CBCT study using surface-based superimposition and deviation analysis. *Clin. Oral Investig.* **2021**, *25*, 2237–2247. [CrossRef] [PubMed]
24. Madhyastha, P.S.; Hegde, S.; Srikant, N.; Kotian, R.; Iyer, S.S. Effect of finishing/polishing techniques and time on surface roughness of esthetic restorative materials. *Dent. Res. J.* **2017**, *14*, 326–330. [CrossRef]
25. Fasbinder, D.J.; Neiva, G.F. Surface Evaluation of Polishing Techniques for New Resilient CAD/CAM Restorative Materials. *J. Esthet. Restor. Dent.* **2016**, *28*, 56–66. [CrossRef]
26. Yilmaz, C.; Korkmaz, T.; Demirköprülü, H.; Ergün, G.; Özkan, Y. Color stability of glazed and polished dental porcelains. *J. Prosthodont.* **2008**, *17*, 20–24. [CrossRef]
27. Anusavice, K.J.; Kakar, K.; Ferree, N. Which mechanical and physical testing methods are relevant for predicting the clinical performance of ceramic-based dental prostheses? *Clin. Oral Implants Res.* **2007**, *18*, 218–231. [CrossRef]
28. Heintze, S.D.; Cavalleri, A.; Forjanic, M.; Zellweger, G.; Rousson, V. Wear of ceramic and antagonist—A systematic evaluation of influencing factors in vitro. *Dent. Mater.* **2008**, *24*, 433–449. [CrossRef]
29. Shaikh, M.Q.; Nath, S.D.; Akilan, A.A.; Khanjar, S.; Balla, V.K.; Grant, G.T.; Atre, S.V. Investigation of Patient-Specific Maxillofacial Implant Prototype Development by Metal Fused Filament Fabrication (MF 3) of Ti-6Al-4V. *Dent. J.* **2021**, *9*, 109. [CrossRef]
30. Asiry, M.A.; AlShahrani, I.; Alaqeel, S.M.; Durgesh, B.H.; Ramakrishnaiah, R. Effect of two-step and one-step surface conditioning of glass ceramic on adhesion strength of orthodontic bracket and effect of thermo-cycling on adhesion strength. *J. Mech. Behav. Biomed. Mater.* **2018**, *84*, 22–27. [CrossRef]
31. Saleeva, L.; Kashapov, R.; Shakirzyanov, F.; Kuznetsov, E.; Kashapov, L.; Smirnova, V.; Kashapov, N.; Saleeva, G.; Sachenkov, O.; Saleev, R. The Effect of Surface Processing on the Shear Strength of Cobalt-Chromium Dental Alloy and Ceramics. *Materials* **2022**, *15*, 2987. [CrossRef] [PubMed]
32. Della Bona, A.; Borba, M.; Benetti, P.; Pecho, O.E.; Alessandretti, R.; Mosele, J.C.; Mores, R.T. Adhesion to Dental Ceramics. *Curr. Oral Health Rep.* **2014**, *1*, 232–238. [CrossRef]
33. Lapinska, B.; Rogowski, J.; Nowak, J.; Nissan, J.; Sokolowski, J.; Lukomska-Szymanska, M. Effect of surface cleaning regimen on glass ceramic bond strength. *Molecules* **2019**, *24*, 389. [CrossRef]
34. Tzanakakis, E.; Kontonasaki, E.; Voyiatzis, G.; Andrikopoulos, K.; Tzoutzas, I. Surface characterization of monolithic zirconia submitted to different surface treatments applying optical interferometry and raman spectrometry. *Dent. Mater. J.* **2020**, *39*, 111–117. [CrossRef] [PubMed]
35. Pantić, M.; Mitrović, S.; Babić, M.; Jevremović, D.; Kanjevac, T.; Džunić, D.; Adamović, D. AFM surface roughness and topography analysis of lithium disilicate glass ceramic. *Tribol. Ind.* **2015**, *37*, 391–399.
36. Kaczmarek, K.; Leniart, A.; Lapinska, B.; Skrzypek, S.; Lukomska-Szymanska, M. Selected spectroscopic techniques for surface analysis of dental materials: A narrative review. *Materials* **2021**, *14*, 2624. [CrossRef]

37. Lapinska, B.; Szynkowska, M.I.; Rogowski, J.; Nowak, J.; Sokolowski, G.; Sokolowski, J.; Lukomska-Szymanska, M. Changes in dental ceramic surface structure and their influence on the bond strength to composite material. *Przem. Chem.* **2017**, *96*, 370–374. [CrossRef]
38. Dutra, D.A.M.; Pereira, G.K.R.; Kantorski, K.Z.; Valandro, L.F.; Zanatta, F.B. Does finishing and polishing of Restorative materials affect bacterial adhesion and biofilm formation? a systematic review. *Oper. Dent.* **2018**, *43*, 37–52. [CrossRef]
39. Lapinska, B.; Szynkowska, M.I.; Szczesio, A.; Domarecka, M.; Sokolowski, J.; Lukomska-Szymanska, M. Lithium silicate ceramic surface properties after surface treatment. *Przem. Chem.* **2017**, *96*, 391–395. [CrossRef]
40. Kreve, S.; dos Reis, A.C. Effect of surface properties of ceramic materials on bacterial adhesion: A systematic review. *J. Esthet. Restor. Dent.* **2022**, *34*, 461–472. [CrossRef]
41. Kozmos, M.; Virant, P.; Rojko, F.; Abram, A.; Rudolf, R.; Raspor, P.; Zore, A.; Bohinc, K. Bacterial adhesion of streptococcus mutans to dental material surfaces. *Molecules* **2021**, *26*, 1152. [CrossRef] [PubMed]
42. Lewandowska, M.; Stefaniuk, T.; Pniewski, J. The technique of measurement of intraocular lens surface roughness using atomic force microscopy. *Interdiscip. J. Eng. Sci.* **2014**, *2*, 21–25.
43. Kara, H.B.; Kara, O.; Sayin, G.; Cakan, U.; Ozturk, A.N. Atomic force microscopy investigation of lithium disilicate glass ceramic after various surface treatments. *Adv. Appl. Ceram.* **2014**, *113*, 301–306. [CrossRef]
44. Tholt, B.; Miranda, W.G.; Prioli, R.; Thompson, J.; Oda, M. Surface roughness in ceramics with different finishing techniques using atomic force microscope and profilometer. *Oper. Dent.* **2006**, *31*, 442–449. [CrossRef]
45. Incesu, E.; Yanikoglu, N. Evaluation of the effect of different polishing systems on the surface roughness of dental ceramics. *J. Prosthet. Dent.* **2020**, *124*, 100–109. [CrossRef]
46. Azevedo, V.L.B.; de Castro, E.F.; Bonvent, J.J.; de Andrade, O.S.; Nascimento, F.D.; Giannini, M.; Cavalli, V. Surface treatments on CAD/CAM glass–ceramics: Influence on roughness, topography, and bond strength. *J. Esthet. Restor. Dent.* **2021**, *33*, 739–749. [CrossRef]
47. Dal Piva, A.M.O.; Contreras, L.P.C.; Ribeiro, F.C.; Anami, L.C.; Camargo, S.E.A.; Jorge, A.O.C.; Bottino, M.A. Monolithic ceramics: Effect of finishing techniques on surface properties, bacterial adhesion and cell viability. *Oper. Dent.* **2018**, *43*, 315–325. [CrossRef]
48. Matthias, K.; Helmut, K.; Rudolf, S.J. The all-porcelain, resin-bonded bridge. *Quintessence Int.* **1991**, *22*, 257–262.
49. Contreras, L.P.C.; Dal Piva, A.M.O.; De Camargo Ribeiro, F.; Anami, L.C.; Camargo, S.E.A.; Jorge, A.O.C.; Bottino, M.A. Effects of manufacturing and finishing techniques of feldspathic ceramics on surface topography, biofilm formation, and cell viability for human gingival fibroblasts. *Oper. Dent.* **2018**, *43*, 593–601. [CrossRef]
50. Hjerppe, J.; Rodas, S.; Korvala, J.; Pesonen, P.; Kaisanlahti, A.; Özcan, M.; Suojanen, J.; Reunanen, J. Surface roughness and streptococcus mutans adhesion on metallic and ceramic fixed prosthodontic materials after scaling. *Materials* **2021**, *14*, 1027. [CrossRef]
51. Delvallée, A.; Oulalite, M.; Crouzier, L.; Ducourtieux, S.; Lambeng, N.; Amor, W.; Bouzakher Ghomrasni, N.; Feltin, N.; Viot, A.; Jamet, C. Correlation of AFM/SEM/EDS Images to Discriminate Several Nanoparticle Populations Mixed in Cosmetics. *Micros. Today* **2021**, *29*, 46–51. [CrossRef]
52. Sidhu, G.K.; Kaushik, A.K.; Rana, S.; Bhansali, S.; Kumar, R. Photoluminescence quenching of Zirconia nanoparticle by surface modification. *Appl. Surf. Sci.* **2015**, *334*, 216–221. [CrossRef]
53. Sharma, S.; Cross, S.E.; Hsueh, C.; Wali, R.P.; Stieg, A.Z.; Gimzewski, J.K. Nanocharacterization in Dentistry. *Int. J. Mol. Sci.* **2010**, *11*, 2523–2545. [CrossRef]
54. Orilisi, G.; Tosco, V.; Monterubbianesi, R.; Notarstefano, V.; Özcan, M.; Putignano, A.; Orsini, G. ATR-FTIR, EDS and SEM evaluations of enamel structure after treatment with hydrogen peroxide bleaching agents loaded with nano-hydroxyapatite particles. *PeerJ* **2021**, *9*, e10606. [CrossRef] [PubMed]
55. Dal Piva, A.M.D.O.; Bottino, M.A.; Anami, L.C.; Werner, A.; Kleverlaan, C.J.; Lo Giudice, R.; Famà, F.; da Silva-Concilio, L.R.; Tribst, J.P.M. Toothbrushing Wear Resistance of Stained CAD/CAM Ceramics. *Coatings* **2021**, *11*, 224. [CrossRef]
56. Garza, L.A.; Thompson, G.; Cho, S.H.; Berzins, D.W. Effect of toothbrushing on shade and surface roughness of extrinsically stained pressable ceramics. *J. Prosthet. Dent.* **2016**, *115*, 489–494. [CrossRef]